X-ray-absorption spectroscopy of Nd^{3+}-exchanged β-alumina crystal

F. Rocca
Centro di Fisica degli Stati Aggregati del Consiglio Nazionale delle Ricerche e Istituto Trentino di Cultura, I-38050 Povo, Trento, Italy

A. Kuzmin and J. Purans
Institute of Solid State Physics, University of Latvia, LV-1063 Riga, Latvia

G. Mariotto
Istituto Nazionale per la Fisica della Materia and Dipartimento di Fisica, Università di Trento, I-38050 Povo, Trento, Italy

(Received 5 July 1995)

The results of x-ray-absorption spectroscopy investigations of Nd^{3+} ions in a nearly fully exchanged (93%) sodium β-alumina crystal are reported. The Nd^{3+} local environment is reconstructed using a multishell best fit procedure and is compared with existing structural models. The experimental extended x-ray-absorption fine-structure (EXAFS) spectra are also compared with model *ab initio* FEFF6 calculations based on the x-ray-diffraction data for the Nd^{3+} ions located at the BR($2d$) and interstitial $A(6h)$ sites of β-alumina. Neodymium ions are mainly found near the BR($2d$) sites of the conduction plane, where they are strongly bonded to three O(5) oxygens located in the same plane and shifted by ~ 0.6 Å from the crystallographic positions occupied in sodium β-alumina. The atoms located at the spinel blocks below and above the conduction plane produce negligible contribution to the total Nd L_3 edge EXAFS signal due to the polarization effect and, mainly, to thermal and/or static disorder. The similarity of the local structure around the Nd^{3+} ions in the β- and β''-alumina crystals is also discussed.

I. INTRODUCTION

Sodium β-alumina is the parent material of a wide family of superionic conductors showing very interesting two-dimensional transport properties even at moderate temperature. Its crystal structure ($P6_3/mmc$ space group), extensively investigated since the early 1970s,[1,2] consists of compact spinel-type blocks of Al_2O_3 interspersed by low atom density layers (conduction planes), where the diffusion of the mobile sodium cations occurs. Two adjacent spinel blocks are held together by columnar Al-O(5)-Al bonds, with the bridging oxygens O(5) forming a honeycomb lattice, where the sodium ions can randomly occupy three different sites (see Fig. 1): Beevers-Ross (BR), anti-Beevers-Ross (aBR), and midoxygen (mid-O) sites. Moreover, significant displacements of sodium ions along the conduction pathways from the lattice positions to the interstitial $A(6h)$ sites have been observed by x-ray-diffraction techniques.[1]

In the past years, the unique ability of β-alumina to exchange the sodium content with a large variety of cations has been exploited, aiming to incorporate in the conduction plane a relevant amount of optically active ions. Although the diffusion rate of trivalent lanthanide ions in this crystal structure is very low even at intermediate temperature, Tietz *et al.*[3] were recently successful in exchanging neodymium in sodium β-alumina crystals, thus opening the door to investigation of the optoelectronic properties of this material.

X-ray-diffraction (XRD) studies[3] show that at high extent of exchange, the Nd^{3+} ions occupy preferentially BR($2d$) sites (95%); a small part (5%) of the Nd^{3+} ions occupies the so-called $A(6h)$ sites which are located ~ 1 Å far from the BR site along the conduction pathways (see Fig. 1). Moreover, XRD suggests that the local environment of neodymium is highly distorted: the O(5) oxygen atoms are shifted from their ideal crystallographic positions occupied in sodium β-alumina so that the Nd-O(5) distance turns out ~ 0.56 Å shorter.

X-ray-absorption spectroscopy (XAS) can provide more accurate information than XRD about the local distortions and correlations of atomic positions, especially in disordered systems: this is due to the different ways of averaging the structural information.[4] Moreover, in complicated multicomponent compounds, XAS allows us to single out the contributions from atoms of different types by looking at different absorption edges. Therefore the use of XAS seems to be very

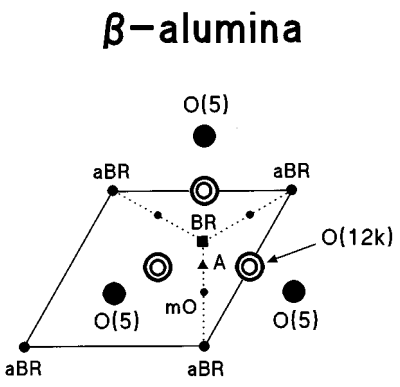

FIG. 1. Local structure of sodium β-alumina: the possible sodium sites (BR, aBR, mid-O, and A) are indicated. The positions of oxygen atoms are shown: O(5) atoms (solid circles) are located in the conduction region; O(12k) atoms (open circles) in the spinel blocks at 2.29 Å above and below the conduction region forming a regular triangular prism.

suitable to study the local structure around the Nd ions in disordered materials such as β- and β''-aluminas.

In a recent paper, we have presented a detailed study of the electronic and crystallographic structure around the Nd^{3+} ions in a 60% Nd-exchanged sodium β''-alumina crystal by the XAS technique applied to a powdered sample.[5] We have found that the neodymium ions are mainly located near the mid-O(9*d*) sites in the conduction plane; they are strongly bonded to two O(5) oxygens which are located in the same plane and are shifted from the crystallographic positions, occupied in sodium β''-alumina crystal, towards the neodymium ions.

In this paper we report on the results of XAS studies at the Nd L_3 edge of a nearly fully Nd-exchanged sodium β-alumina single crystal (with about 93% of sodium content replaced by neodymium).

II. EXPERIMENTAL DETAILS

Single crystals of sodium β-alumina, with actual composition $Na_{1.22}Al_{11}O_{17.11}$, were grown by flux evaporation. A 93% Nd^{3+}-exchanged crystal ($Na_{0.08}Nd_{0.38}Al_{11}O_{17.11}$) was obtained by keeping a platelet in molten $NdCl_3$ at 760 °C for 16 h, as reported in Ref. 3. The extent of exchange was measured by a ^{22}Na radio-tracer diffusion technique. The crystallographic structure of the 93% Nd^{3+}-exchanged sodium β-alumina crystal at 298 K was characterized by single-crystal XRD: it was related to the $P6_3/mmc$ space group with lattice parameters $a=5.5848(8)$ Å and $c=22.406(5)$ Å, respectively.

X-ray-absorption spectra at the Nd L_3 edge were measured in transmission mode at room temperature using the standard setup of the DCI D21 (EXAFS-2) beam line (LURE, France). The synchrotron radiation was monochromatized using a Si(311) double-crystal monochromator. The experimental spectra were recorded in the energy range from 6100 to 6700 eV with an energy step of 2 eV and resolution of $\sim$1.5 eV. Our sample had a thickness x corresponding to an absorption jump $\Delta\mu x \simeq 0.8$ (μ is the absorption coefficient). It was oriented in such a way that the polarization vector of the incoming x-ray beam was parallel to the ab plane. The rotation of the sample around the c axis (the direction of the incoming beam) did not show any detectable polarization dependence of the extended x-ray-absorption fine structure (EXAFS). The theoretical evaluation of the polarization influence on the EXAFS signal suggests that such an effect should be enough small due to the symmetry of the structure.

The EXAFS spectra from a single crystal can be contaminated by Bragg diffraction peaks.[6] To check their possible presence in our case, we have done absorption experiments in transmission mode at slightly different orientations of the c axis of the crystal in respect with the x-ray beam direction. Transmission measurements were also compared with some measurements performed using the total electron yield (TEY) detection technique. All measured spectra were similar within the experimental error, indicating the absence of any detectable Bragg reflection in the EXAFS spectra.

In spite of the similarity, the experimental EXAFS spectra obtained in transmission mode had a better signal-to-noise ratio than those provided by TEY: therefore we have used the former in the further analysis.

III. DATA ANALYSIS

The experimental spectra were analyzed by the EXAFS data analysis software package EDA.[7] The analysis was performed in the same way as for β''-alumina crystal.[5]

In our previous work,[5] we used two reference compounds ($NdCoO_3$ and $NdNiO_3$) to test the reliability of the scattering amplitude and phase shift functions for the Nd-O pair calculated by the FEFF code.[8] $NdAlO_3$, whose chemical composition is more similar to Nd-β-alumina, has been used in the present work as an additional reference compound: this allows us to test also the data for the Nd-Al pair. The structure of $NdAlO_3$ crystal was generated using single-crystal XRD data,[9] and the total Nd L_3-edge EXAFS signal was calculated by the FEFF6 code.[8] The calculations were performed for a cluster of 7 Å radius around the absorbing Nd atom, taking into account all the single and multiple scattering paths up to third order. The complex Hedin-Lundqvist potential was used to approximate the exchange-correlation term. Thermal disorder was introduced through a set of exponential terms $\exp(-2\sigma_i^2 k^2)$ [k is the wave vector of the photoelectron defined as in Ref. 5; see also Fig. 3(c)] where σ_i^2 were found for each i scattering path through a best fit procedure. The results of the calculation are presented in Fig. 2. They are in good agreement with the experimental data in the whole range of analysis ($k<10$ Å^{-1} and $R<7$ Å), supporting the reliability of the theoretical scattering amplitude and phase shift functions utilized to fit the experimental data of the β-alumina crystal.

The experimental x-ray-absorption spectrum μ_{expt} at the Nd L_3 edge in β-alumina is shown in Fig. 3(a). The region corresponding to x-ray-absorption near-edge structure (XANES) is presented in Fig. 3(c) where also the previous spectrum of Nd-exchanged (60%) β''-alumina is shown for comparison. The EXAFS signal was extracted by using the same procedure of Ref. 7, as shown in Figs. 3(a) and 3(b). The background contribution μ_{back} [dotted line in Fig. 3(a)] was first subtracted from the experimental data μ_{expt}. The atomiclike contribution μ_0 (''zero-line'') was subsequently found by a multistep procedure:[7] at the first step, a polynomial of third order, $\mu_0^{(1)}$ [dashed line in Fig. 3(a)], was least-squares fitted to the experimental signal μ_{expt} above the absorption edge. $\mu_0^{(1)}$ gives the first approximation to the zero line and is utilized for the normalization of the edge jump (see below). Further, the correction to the zero line was determined by a combined polynomial-splice technique.[7] Such a sophisticated approach allows us to remove precisely the low-frequency contributions in EXAFS and, thus, to minimize the distortion of the first-shell EXAFS signal. The total zero-line function μ_0, obtained within the multistep procedure, is presented in Fig. 3(b) by a dashed line. Finally, the EXAFS signal $\chi(k)$ was calculated as $\chi=(\mu_{expt}-\mu_{back}-\mu_0)/\Delta\mu$ where $\Delta\mu=\mu_0^{(1)}$ is the edge-jump function. The extracted experimental EXAFS and its Fourier transform (FT) are presented in Figs. 4(a) and 4(b). Note that in all figures the FT's are not corrected for the photoelectron phase shift; therefore the positions of peaks differ from the true

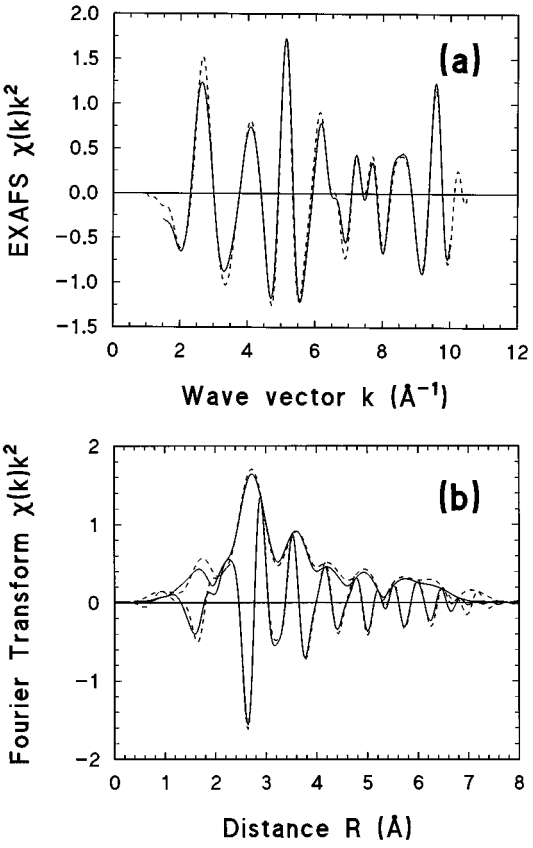

FIG. 2. (a) Experimental (dashed line) and calculated (solid line) EXAFS $\chi(k)k^2$ of the Nd L_3 edge in $NdAlO_3$. (b) Modulus and imaginary part of the Fourier transformed spectra shown in (a).

crystallographic values. As one can see, the EXAFS signals in both aluminas are close [Fig. 4(a)]; however, the EXAFS of β-alumina crystal has more intense fine structures in the range 3.0–5.5 $Å^{-1}$.

As in the case of the Nd L_3-edge EXAFS in a Nd-exchanged (60%) sodium β''-alumina crystal, we have found here too the strong contribution due to the atomic x-ray-absorption fine structure[10] (AXAFS) [see the μ_0 peak in Fig. 4(b)]. It was determined and subtracted from the experimental signal as previously done.[5] After elimination of the AXAFS signal, two main contributions, related to the first three peaks, can be singled out by the back FT in the intervals 0.6–3.6 Å and 3.6–5.1 Å, respectively (Fig. 5). A brief overlook of the amplitude behavior of these two signals allowed us to conclude (remembering the different backscattering amplitude behavior of oxygen and aluminum atoms) that the first signal originates from a complex coordination shell, while the second one is mainly due to the aluminum atoms. The FT signal was back-Fourier transformed in the extended range $R=0.6$–5.1 Å: in this way the EXAFS signal related to the main contributions was singled out and used in the final best fit procedure. Three peaks, located at ~2.0, ~3.0, and ~4.2 Å in the FT of the experimental EXAFS spectrum [Fig. 6(b)], contribute in this range: therefore a three-shell model, containing oxygen atoms (for the first peak) and aluminum atoms (for the outer two peaks), was used as the first approximation. However, a detailed analysis showed that the last peak at ~4.2 Å has a more complex origin, due to the groups of aluminum and oxygen

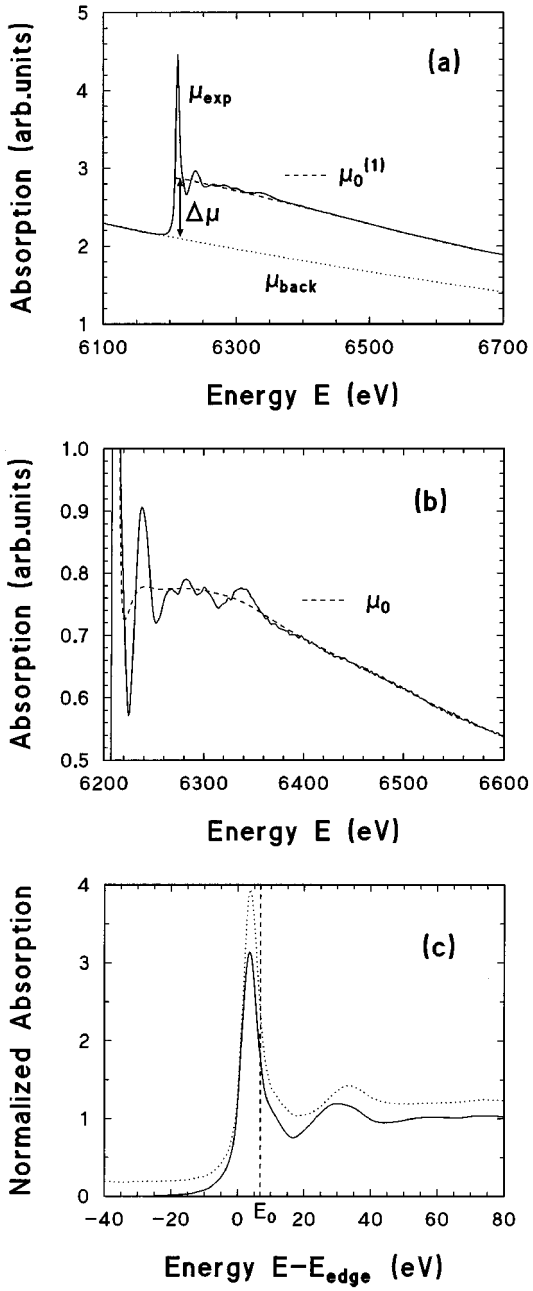

FIG. 3. (a) Experimental x-ray-absorption spectrum μ_{expt} (solid line) at the Nd L_3 edge in a Nd^{3+}-exchanged (93%) sodium β-alumina crystal. The initial steps of the EXAFS extraction procedure are shown: μ_{back} (dotted line) is the background contribution; $\mu_0^{(1)}$ (dashed line) is the first-step zero line related to the atomiclike contribution and used in the normalization procedure of the EXAFS function (see text for details); $\Delta\mu$ is the edge-jump function. (b) Background-subtracted experimental spectrum $\mu_{expt}-\mu_{back}$ (solid line) and the total zero line μ_0 (dashed line) obtained by the multistep procedure described in text. (c) Normalized experimental XANES spectra of the Nd L_3 edge in a Nd^{3+}-exchanged (93%) sodium β-alumina crystal (solid line) and in a Nd^{3+}-exchanged (60%) sodium β''-alumina crystal (Ref. 5) (dotted line). E_{edge} is equal to 6207.9 eV. The position of the photoelectron energy origin E_0, related to the continuum threshold, is shown by a dashed line. For clarity the dotted spectrum has been upwards shifted.

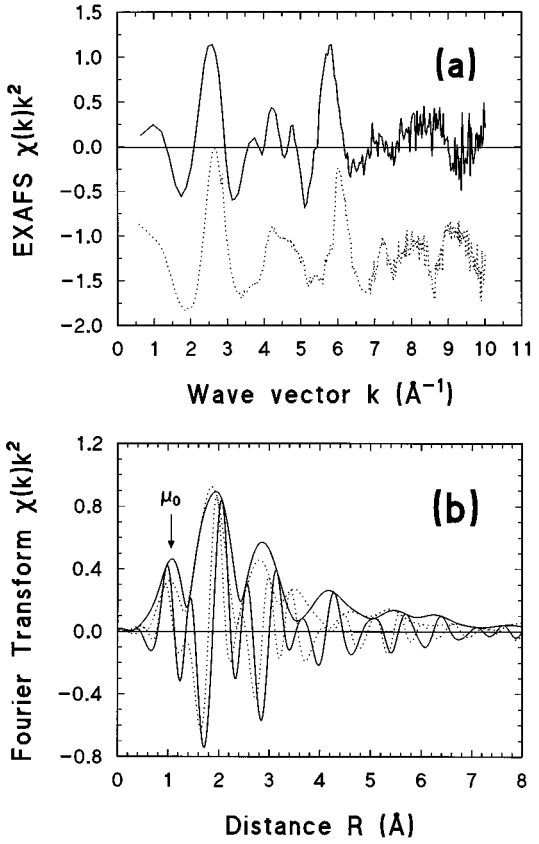

FIG. 4. (a) Experimental EXAFS $\chi(k)k^2$ of the Nd L_3 edge in a Nd^{3+}-exchanged (93%) sodium β-alumina crystal (solid line) and in a Nd^{3+}-exchanged (60%) sodium β''-alumina crystal (Ref. 5) (dotted line). (b) Modulus and imaginary part of the Fourier-transformed spectra shown in (a). The position of the AXAFS contribution (μ_0) is shown by an arrow.

atoms located in the outer shells. Finally, we found that the use of a four-shell model gives the best agreement with experiment. Note that the inclusion of the fourth shell, containing oxygen atoms, does not influence the structural parameters obtained for the first two shells and only slightly modifies the parameters of the third shell.

The result of the best fit analysis of the EXAFS function (performed in the range $k=1.5$–10.0 $Å^{-1}$) is shown in Fig. 6. A summary of the obtained results is presented in Table I. We used 12 fitting parameters [three (N,R,σ^2) for each shell], which is much smaller than the number of independent data points, $N_{\rm ind}=24$ ($N_{\rm ind}\approx 2\Delta k\Delta R/\pi$ where Δk and ΔR are, respectively, the widths in k and R space used in the fit[11]).

Note that the values of the coordination numbers presented in Table I are not corrected for the polarization influence, and do not correspond to the true coordination numbers. In fact, EXAFS measured in single crystals should be more carefully analyzed, because the polarization effects are not spherically averaged. In our case, the contribution of the atoms in the conduction plane is amplified with respect to that of the atoms in the spinel blocks. On the contrary, the rotation of the sample around c axis (i.e., the direction of the incoming beam) does not show any detectable polarization dependence of the Nd L_3-edge EXAFS.

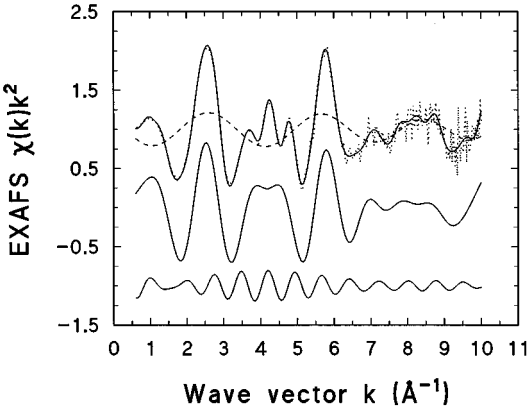

FIG. 5. Experimental EXAFS $\chi(k)k^2$ of the Nd L_3 edge in a Nd^{3+}-exchanged (93%) sodium β-alumina crystal (dotted line) and the same signal after Fourier filtration in the range from 0 to 8 Å (upper solid line). The AXAFS signal is shown by a dashed line. The lower two solid lines correspond to the contributions from the first three peaks extracted by the back FT in the intervals 0.6–3.6 Å and 3.6–5.1 Å. For clarity all the spectra have been vertically shifted.

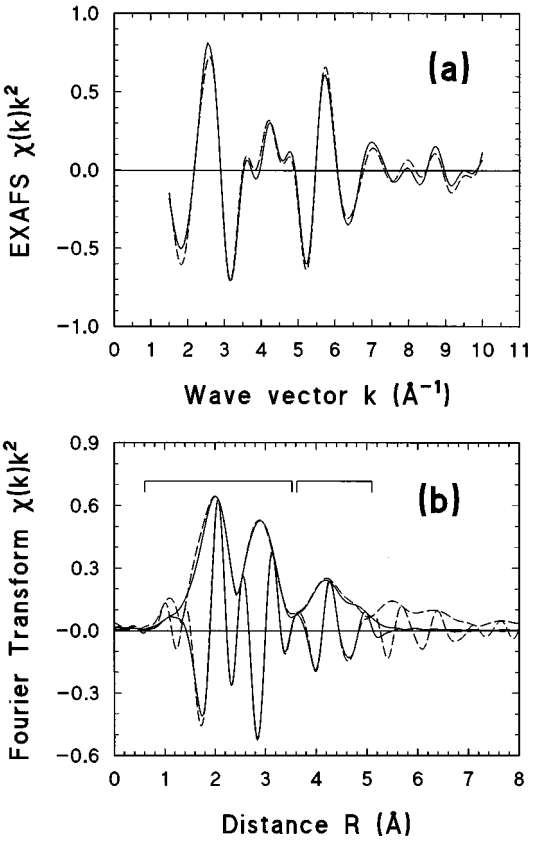

FIG. 6. (a) The experimental EXAFS signal (dashed line) singled out in the range 0.6–5.1 Å and its best fit (solid line). (b) The FT of the best fit signal shown in (a) (solid line) in comparison with the FT of the total experimental EXAFS signal (dashed line). The intervals corresponding to two contributions shown in Fig. 5 are indicated.

TABLE I. Structural data obtained from the best fit analysis of the Nd L_3 edge EXAFS (see Fig. 6) and from x-ray single-crystal diffraction (N is the number of atoms located at the distance R from the neodymium, and σ^2 is the Debye-Waller factor). Note that the values of coordination numbers obtained by EXAFS are not corrected for the polarization influence. The groups of oxygen atoms located in the conduction plane are marked by an asterisk.

	EXAFS			XRD [3]			
				95% Nd in the BR($2d$) site		5% Nd in the $A(6h)$ site	
	N	R (Å)	σ^2 (Å^2)	N	R (Å)	N	R (Å)
O						2*	2.33
O	4±1	2.63±0.02	0.01±0.005	3*	2.66	4	2.68
O				6	2.79		
Al						2	3.25
Al						4	3.29
O						2* + 2	3.30
O						2	3.44
Al				6	3.57		
Al	6±1	3.51±0.03	0.02±0.005	6	3.61		
O						1*	3.64
Al						4	3.91
O				6	4.02		
O						4	4.27
O				2	4.34		
O						2	4.45
Al						2	4.51
O						2* + 4	4.51
Al						4	4.63
O	3±2	4.7±0.05	0.003±0.005	12	4.86	8	4.84
O				12	5.28	2*	5.21
Al	10±3	5.4±0.05	0.02±0.005	12	5.33		
O						8	5.38
Al						4	5.57

The experimental EXAFS signal has been also compared to the model *ab initio* calculations for the Nd ions located at the BR($2d$) and $A(6h)$ crystallographic sites.[3] The calculations were performed by the FEFF6 code[8] using the same set of parameters optimized for $NdAlO_3$ (see above) and a fixed set of atomic positions given by XRD (Ref. 3) for the BR($2d$) and $A(6h)$ sites. The influence of thermal and static disorder was approximated by an average damping term $\exp(-2\sigma^2k^2)$ with $\sigma^2=0.012$ Å^2. Since we were interested in checking the correctness and accuracy of interatomic distances given by XRD, a comparison between the frequencies of the experimental and calculated EXAFS signals was a top priority. The polarization influence was correctly taken into account[8] for the orientation of the crystal in respect to the polarization vector of the incoming x-ray beam. The result of the calculations is shown in Fig. 7. It is clear that the simple use of the atomic coordinates provided by XRD (Ref. 3) without any fitting parameters leads to the conclusion that the location of neodymium ions in the BR($2d$)-type site is more likely than in the $A(6h)$-type site. Note that performing a set of calculations at different orientations of the polarization vector, we observed that the influence of the polarization effects on the EXAFS signals is much smaller than the difference between the calculated EXAFS signals for the Nd ions in the BR($2d$) and $A(6h)$ sites.

IV. DISCUSSION

The x-ray-absorption spectrum at the Nd L_3 edge in β-alumina consists of a prominent peak, the so-called ''white line'' (WL), and the EXAFS above it [Fig. 3(c)]. The WL is located below the continuum threshold and corresponds to the transition from the core state $2p_{3/2}$(Nd) to quasibound states having the $5d$(Nd) atomic character.[5] The XANES region of β- and β''-aluminas is similar except that a small difference is present in the WL amplitudes, and the frequency of the EXAFS oscillation above the WL is slightly higher in the case of β-alumina [the position of the maximum at $\sim$30–35 eV in Fig. 3(c) is closer to the E_0 reference value]. The WL amplitude, the first difference, depends strongly on the experimental resolution, which was different for these two measurements, and on the polarization influence on the XANES signal. The second difference indicates that longer distances are present in the first shell of β-alumina. This fact is in good agreement with XRD results: the average Nd-O distance in the first shell is 2.69 Å in

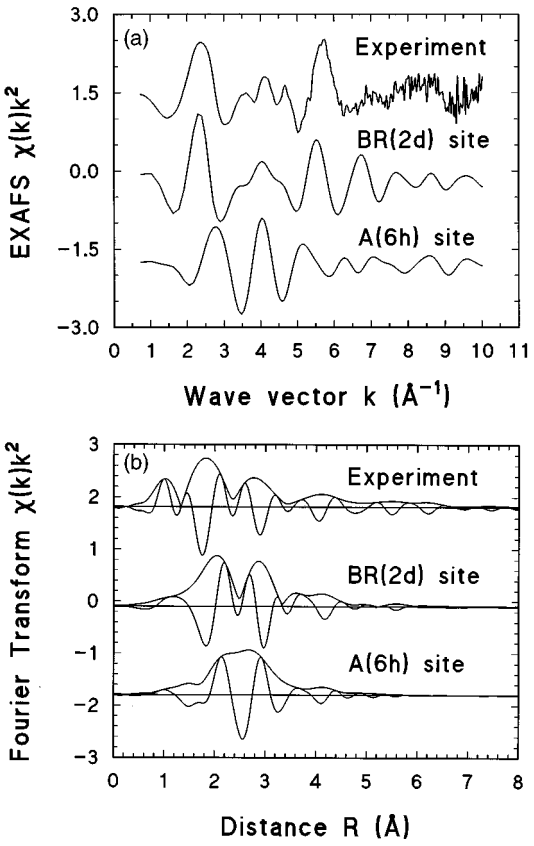

FIG. 7. (a) Comparison of the experimental EXAFS $\chi(k)k^2$ of the Nd L_3 edge in a Nd^{3+}-exchanged (93%) sodium β-alumina crystal with the results of *ab initio* FEFF6 calculations based on the XRD data for the Nd ions located at the BR(2*d*) and $A(6h)$ sites, respectively. (b) The FT's of the EXAFS signals presented in (a).

β''-alumina[12] and 2.75 Å in β-alumina.[3] The small difference between the positions of the first-shell peak at about 1.8 Å in two aluminas is also visible in the FT's of their EXAFS signals [Fig. 4(b)].

The best fit of the experimental EXAFS signal (Fig. 6) allowed us to obtain a set of structural parameters describing the local environment around the Nd ions (Table I). Four groups of atoms were found: the oxygens at 2.63 and 4.74 Å and the aluminums at 3.51 and 5.39 Å. The obtained atomic positions agree better with the location of neodymium at the BR(2*d*) site rather than at the $A(6h)$ site: this is opposite to the case of β''-alumina where the Nd^{3+} ions occupy preferentially the mid-O(9*d*) sites.[5] However, in both cases the Nd^{3+} ions have similar local environments consisting of eight (or nine) oxygen atoms: three oxygen ions up and three down in the spinel-type blocks at the distance $\sim$2.70–2.79 Å plus two (or three) neighbors located at $\sim$2.46–2.66 Å in the conduction plane.

The difference between EXAFS spectra for neodymium ions located at the BR(2*d*) and $A(6h)$ sites can be seen from the results of the *ab initio* EXAFS calculations shown in Fig. 7 (see Sec. III for details of the calculations). It is clear that the calculated signals differ significantly both in k and R space and that EXAFS of Nd-exchanged β-alumina shows a distortion of the local structure in comparison with that of ''true'' crystallographic sites. The results obtained with the best fit (see Fig. 6 and Table I) give the best agreement with the experiment and allow one to specify the XRD data.[3] As a result, one has that the shortest obtained distances, attributed to the Nd-O(5) and Nd-Al(3) pairs, are slightly shortened by 0.03 and 0.10 Å, respectively, compared to the crystallographic parameters of sodium β-alumina.[3]

Note that some groups of nearest atoms located in the spinel-type blocks above and below the Nd^{3+} ions were not detected. This might be due to the influence of the polarization effect and/or to the high disorder (thermal and/or static) which increases the Debye-Waller (DW) factor. Our polarization-dependent calculations by the FEFF6 code[8] show that even under the highest influence of the polarization effect, the contribution from the atoms of the spinel-type blocks should be present in the total EXAFS signal. In fact, the complete disappearance, due to the polarization effect, of an atomic contribution can be observed only for K edge absorption when the angle between the polarization vector and the direction toward a group of atoms is equal to 90°. In our case, we deal with L_3 edge absorption and no group of atoms forming the 90° angle with the polarization vector is present in the local surroundings of neodymium within the spinel-type blocks. Thus, we conclude that the main reason why these atoms are not detectable is the high thermal disorder.

It is interesting to point out that also for the β''-alumina the oxygen atoms O(5), located in the conduction planes, are better detectable by EXAFS than the ones of the spinel-type blocks.[5] Previously, we attributed this effect to evidence of the correlation in the vibrational motion of neodymium with oxygens O(5) and aluminums Al(6c) connected to them contrary to other outer groups of atoms. It seems that this explanation also holds for β-alumina crystal. A similar influence of the vibrational correlation was found by single-crystal XRD in potassium β-alumina by Dernier and Remeika:[13] it was suggested that definite correlations exist between the O(5) atoms and the potassium ions diffusing in the plane. Even larger correlation effects were also suggested for bigger ions, like rubidium:[13] therefore the occurrence of a vibrational correlation in Nd-exchanged sodium β-alumina is not surprising.

Let us now consider the behavior of the displacement correlation function (DCF) σ^2_{DCF}, which is equal to the difference between the thermal mean square relative displacement (MSRD) $\sigma^2_{\mathrm{MSRD_{th}}}$ and the thermal mean square displacement (MSD) $\sigma^2_{\mathrm{MSD_{th}}}$. A good estimate of the correlation can be the ratio $\gamma=\sigma^2_{\mathrm{DCF}}/\sigma^2_{\mathrm{MSD_{th}}}$ with $\gamma=1$ for completely correlated motion and $\gamma=0$ in the opposite case.[14] However, in general case, the σ^2_{MSRD} obtained from the EXAFS DW factor and the σ^2_{MSD} obtained from the XRD DW factor contain the contributions from both static ($\sigma^2_{\mathrm{MSRD_{st}}}$ and $\sigma^2_{\mathrm{MSD_{st}}}$) and thermal ($\sigma^2_{\mathrm{MSRD_{th}}}$ and $\sigma^2_{\mathrm{MSD_{th}}}$) disorder, with $\sigma^2_{\mathrm{MSRD_{st}}}\simeq\sigma^2_{\mathrm{MSD_{st}}}$. Therefore, for the experimental data on σ^2_{MSRD} and σ^2_{MSD}, one has

$$\gamma\simeq\frac{\sigma^2_{\mathrm{MSD_{th}}}-\sigma^2_{\mathrm{MSRD_{th}}}}{\sigma^2_{\mathrm{MSD_{th}}}+\sigma^2_{\mathrm{MSD_{st}}}}. \tag{1}$$

For the Nd-O(5) atom pair, σ^2_{MSRD} is about 0.012 $\mathrm{Å}^2$ (see Table I) and σ^2_{MSD} is about 0.05 $\mathrm{Å}^2$ (see Ref. 3) and thus the

value of $\gamma \simeq 0.8$ is high if static disorder is present. If static disorder is absent ($\sigma^2_{\mathrm{MSD}_{st}} = 0$), the value of γ will be even higher. Thus the comparison of the EXAFS and XRD DW factors allows us to recognize the presence of a highly correlated motion. The reason for the high correlation of atomic motion of neodymium and O(5) oxygens located in the conduction plane is the strength of the Nd-O(5) short bond.[15] This result implies a much tighter binding of Nd^{3+} ions compared to Na^{+} ions in β-alumina, which is consistent with the result that sodium β-alumina is a much better conductor than Nd-exchanged sodium β-alumina.

V. CONCLUSIONS

In this work, we have presented an x-ray-absorption spectroscopy study of the Nd^{3+} L_3 edge in a 93% Nd-exchanged sodium β-alumina single crystal. On the grounds of a multishell best fit analysis and *ab initio* calculations of EXAFS for different possible sites of neodymium, we can conclude that neodymium ions are mainly located near the BR($2d$) sites of the conduction region; they are strongly bonded to three O(5) oxygens which are located in the same plane and shifted from the crystallographic positions occupied in sodium β-alumina crystal by ~ 0.60 Å. The reason for the high correlation of atomic motion of neodymium and oxygen atoms in the conduction plane is the strength of the Nd-O(5) short bond.

The absence in the Nd L_3 edge EXAFS of any detectable contribution from nearest atoms of the spinel-type blocks (located below and above the conduction plane) is mainly due to thermal and/or static disorder, which leads to very rapid amplitude damping of the EXAFS signals from these atoms.

ACKNOWLEDGMENTS

The authors wish to thank Dr. S. Benazeth, Dr. R. Cortes, and the staff of the LURE laboratory for support during the experiments. They are thankful to Dr. F. Tietz for providing them with the β-alumina sample and for fruitful discussions. Finally, they are grateful to Professor T. Isihara for providing the $NdAlO_3$ sample. A.K. and J.P. wish to thank the Consiglio Nazionale delle Ricerche (Italy) and the Università di Trento for hospitality and financial support. This work was supported in part by the International Science Foundation, under Grant Nos. LF8000 and LJ8100, and by the Italian Consiglio Nazionale delle Ricerche, under Contract No. 93.01312.CT02.

[1] C. R. Peters, M. Bettman, J. W. Moore, and M. D. Glick, Acta Crystallogr. B **27**, 1826 (1971).

[2] K. Edström, J. O. Thomas, and G. C. Farrington, Acta Crystallogr. B **47**, 210 (1991).

[3] F. Tietz, Ph.D. thesis, Universität Hannover, 1992; F. Tiez and W. Urland, J. Solid State Chem. **100**, 255 (1992).

[4] B. Rechav, Y. Yacoby, E. A. Stern, J. J. Rehr, and N. Newville, Phys. Rev. Lett. **72**, 1352 (1994).

[5] F. Rocca, A. Kuzmin, J. Purans, and G. Mariotto, Phys. Rev. B **50**, 6662 (1994).

[6] K. H. Kim, W. T. Elam, E. F. Skelton, J. P. Kirkland, and R. A. Neiser, Phys. Rev. B **42**, 10 724 (1990).

[7] A. Kuzmin, Physica B **208&209**, 175 (1995).

[8] J. J. Rehr, J. Mustre de Leon, S. I. Zabinsky, and R. C. Albers, J. Am. Chem. Soc. **113**, 5135 (1991); J. Mustre de Leon, J. J. Rehr, S. I. Zabinsky, and R. C. Albers, Phys. Rev. B **44**, 4146 (1991).

[9] M. Marezio, P. D. Dernier, and J. P. Remeika, J. Solid State Chem. **4**, 11 (1972).

[10] B. W. Holland, J. B. Pendry, R. F. Pettifer, and J. Bordas, J. Phys. C **11**, 633 (1978); S. I. Zabinsky, Ph.D. thesis, University of Washington, 1993; J. J. Rehr, C. H. Booth, F. Bridges, and S. I. Zabinsky Phys. Rev. B **49**, 12 347 (1994).

[11] Report on the International Workshop on Standards and Criteria in XAFS, in *X-Ray Absorption Fine Structure*, edited by S. S. Hasnain (Ellis Horwood, New York, 1991), p. 751.

[12] W. Carrillo-Cabrera, J. O. Thomas, and G. C. Farrington, Solid State Ion. **28–30**, 317 (1988).

[13] P. D. Dernier and J. P. Remeika, J. Solid State Chem. **17**, 245 (1976).

[14] W. Bohmer and P. Rabe, J. Phys. C **12**, 2465 (1979).

[15] G. Dalba, P. Fornasini, F. Rocca, and S. Mobilio, Phys. Rev. B **41**, 9668 (1990).